# Electroreflectance intensity for resonant coupling between Wannier-Stark localization states in a GaAs/AlAs superlattice

Isao Tanaka, Masaaki Nakayama, and Hitoshi Nishimura
*Department of Applied Physics, Faculty of Engineering, Osaka City University, Sugimoto, Sumiyoshi-ku, Osaka 558, Japan*

Kenji Kawashima
*ATR Optical and Radio Communications Research Laboratories, Seika-cho, Soraku-gun, Kyoto 619-02, Japan*

Kenzo Fujiwara
*Department of Electrical Engineering, Kyushu Institute of Technology, Tobata-ku, Kitakyushu, Fukuoka 804, Japan*
(Received 3 March 1992)

We have measured the electric-field dependence of the electroreflectance intensities of the heavy-hole and light-hole exciton transitions associated with the first ($n=1$) subbands in a GaAs (6.4 nm)/AlAs (0.9 nm) superlattice embedded in a *p-i-n* structure at 77 K. It is found that the electroreflectance intensities are highly sensitive probes to detect the resonant couplings between the Wannier-Stark localization states owing to the intensity reduction induced by the wave-function delocalization. We have clearly detected the various resonant couplings between the hole subbands, which have not been observed yet, in addition to those between the electron subbands. We have analyzed the electroreflectance-intensity change for the resonant coupling on the basis of the overlap integral between the electron and hole wave functions by using a transfer-matrix method with the Airy function.

## I. INTRODUCTION

Recently, the electric-field-induced localization of the extended wave function, Wannier-Stark (WS) localization, in semiconductor superlattices (SL's) has been extensively studied because of the fundamental interest in experimental[1-11] and theoretical[12-16] aspects and the application of electro-optic devices.[17,18] The WS localization results in the quantization of the energy continuum into the Stark ladders of the discrete energy levels with an equal energy spacing of $eFD$: the energy of the interband transition, so called Stark-ladder transition, is given by $E_0+meFD$ ($m=0,\pm1,\pm2,\ldots$), where $E_0$ is an interband transition energy in an isolated quantum well (QW), $F$ is an electric field, $D$ is a SL period, and $m$ is a Stark-ladder index indicating an oblique transition in real space. The oscillator strengths of the Stark-ladder transitions depend on the extent of the wave-function localization. Although there is a long-standing controversy as to whether or not the WS localization is an exact solution of a periodic Hamiltonian in the presence of an external electric field,[14-16] it is not within the scope of this paper.

In our previous work [electroreflectance (ER) measurements][9] and Refs. 6 and 11 [photocurrent (PC) measurements], it is clearly indicated that when the energy of $meFD$ just agrees with the energy spacing between the first ($n=1$) and $n=2$ electron subbands ($meFD=\Delta E_{12}$), the WS localization state of the $n=1$ electron subband in a QW resonantly couples with that of the $n=2$ subband in the $m$th-nearest-neighbor QW (lower potential side). We found that the resonant coupling appears as not only the splitting features of the ER-line shapes due to the formation of the bonding and antibonding states but also the reduction of the ER intensities of the related Stark-ladder transitions due to the wave-function delocalization.[9] Although the splitting features are observed for the first-nearest-neighbor resonant coupling between the $n=1$ and $n=2$ electron subbands in the PC spectra,[6,11] we have demonstrated that ER spectroscopy is much more sensitive to detect the resonant coupling than PC spectroscopy.[9] While the resonant coupling of electrons has been investigated extensively,[6,9-11] there is no report on the resonant coupling of holes in SL's. In asymmetric double-QW structures, the resonant coupling between the hole states has been studied by photoluminescence spectroscopy.[19,20]

In the present work, we have investigated the resonant coupling between the WS localization states in a GaAs (6.4 nm)/AlAs (0.9 nm) SL by measuring the electric-field dependence of the ER intensities of the heavy-hole and light-hole exciton transitions associated with the $n=1$ subbands. In the ER spectra, it is easy to observe the intensity change because of the flatness of the base line. On the other hand, in PC spectroscopy, which has been a major method for investigating the WS localization, it is difficult to observe the intensity change because the PC spectra include broad absorption bands as a background. From the ER-intensity change as a function of electric field, we have clearly detected the second-, third-, and fourth-nearest-neighbor resonant couplings between the $n=1$ and $n=2$ electron subbands, the first-nearest-neighbor resonant coupling between the $n=1$ and $n=2$ ($n=3$) heavy-hole subbands, and the first-, second-, and third-nearest-neighbor resonant couplings between the $n=1$ and $n=2$ light-hole subbands. We discuss the ER-intensity change for the resonant coupling on the basis of the overlap integral between the electron and hole wave functions by using a transfer-matrix (TM) method.

 

## II. EXPERIMENT

The sample of the GaAs (6.4 nm)/AlAs (0.9 nm) SL was grown on an $n$-type (Si-doped) (001) GaAs substrate by molecular-beam epitaxy. The SL has 20 periods and is placed in the center of a $p$-$i$-$n$ diode structure, where the $n$ and $p$ layers are Si-doped ($\sim 1\times 10^{18}$ cm$^{-3}$) and Be-doped ($\sim 1\times 10^{19}$ cm$^{-3}$) $Al_{0.33}Ga_{0.67}As$ layers with a 0.8-$\mu$m thickness, respectively. It was determined that the SL period is 7.39 nm by a small-angle x-ray-diffraction method.[4] The sample was processed into a mesa structure with $\sim$400-$\mu$m diam. A windowed gold film with $\sim$250-$\mu$m-diam open area and a 300-nm thickness was evaporated onto the 30-nm $p^+$-type GaAs capping layer for Ohmic contact formation. The ER measurements were performed at 77 K. The probe light was produced by combination of a halogen lamp (50 W) and a monochromator with 0.5-nm resolution. The reflected light was detected with a Si photodiode. The electric field was modulated with the amplitude of 20 mV and the frequency of 210 Hz around a given dc bias. The ER signals were obtained by a conventional lock-in technique.

## III. TRANSFER-MATRIX METHOD AND CALCULATED RESULTS

We first present the calculated results of the energies of the WS localization states as a function of electric field by using the TM method proposed by Hutchings.[21] Transforming the SL growth coordinate $z$ to the dimensionless coordinate $Z_j$ in the Schrödinger equation for an applied electric field $F$,

$$Z_j=-[2m_j/(e\hbar F)^2]^{1/3}(E-V_j+qFz)\ , \tag{1}$$

we obtain the following TM relation from the wave-function continuity at the interface between the $j$th and $(j+1)$th layers:

$$\begin{bmatrix} \mathrm{Ai}(Z_j) & \mathrm{Bi}(Z_j) \\ m_j^{-2/3}\mathrm{Ai}'(Z_j) & m_j^{-2/3}\mathrm{Bi}'(Z_j) \end{bmatrix} \begin{bmatrix} a_j \\ b_j \end{bmatrix} = \begin{bmatrix} \mathrm{Ai}(Z_{j+1}) & \mathrm{Bi}(Z_{j+1}) \\ m_{j+1}^{-2/3}\mathrm{Ai}'(Z_{j+1}) & m_{j+1}^{-2/3}\mathrm{Bi}'(Z_{j+1}) \end{bmatrix} \begin{bmatrix} a_{j+1} \\ b_{j+1} \end{bmatrix}, \tag{2}$$

where $m_j$ and $V_j$ are the effective mass and potential in the $j$th layer, respectively, $q=-e$ $(+e)$ for electrons (holes), and Ai and Bi are the Airy functions. The boundary conditions is $(a_f,b_f)=(1,0)$ for $Z_f\to\infty$ because $\mathrm{Ai}(\infty)\to 0$ and $\mathrm{Bi}(\infty)\to\infty$, and the wave-function transmittance is given by $T=1/(a_i^2+b_i^2)$, where the subscripts $i$ and $f$ indicate the initial and final media, respectively. We assume that the energies of the transmittance maxima correspond to those of quasibound states. In the present calculation, the sample is approximated by a system of eleven QW's sandwiched by semi-infinite AlAs layers corresponding to the initial and final media. In the analysis of the resonant coupling, the energy spacing between the $n=1$ and higher subbands is one of the most important factors; however, the confinement energy of the higher subband is sensitive to the inaccuracy of the layer thicknesses in the sample preparation and the effective-mass parameters in the calculation. We treat the effective-masses and the band nonparabolicities (i.e., the electron, heavy-hole, and light-hole effective masses $m_e$, $m_{hh}$, and $m_{lh}$, respectively, and the band nonparabolicity factors $\gamma_e$ and $\gamma_{lh}$) as adjustable parameters to fit the calculated results to the experimental results described in the next section. We use the following parameters: for GaAs, $m_e=0.0665$, $m_{hh}=0.5$, and $m_{lh}=0.117$; for AlAs, $m_e=0.15$, $m_{hh}=0.6$, and $m_{lh}=0.18$; $\gamma_e$ (GaAs)$=2.7\times 10^{-19}$ m$^2$ and $\gamma_{lh}$ (GaAs)$=0.6\times 10^{-19}$ m$^2$, where we take into account the band nonparabolicity according to Ref. 22. We assume that the conduction-band-offset ratio is 0.66.

Figure 1 shows the calculated energies of the WS localization states of (a) electrons, (b) heavy holes, and (c) light holes in the GaAs (6.4 nm)/AlAs (0.9 nm) SL as a function of electric field. Since the base line of the SL potential is in proportion to the growth coordinate under the electric field, $eFz$, the energies are measured with respect to the center of the sixth QW corresponding to the center of the modeled SL with the eleven QW's. The notations of $En(\pm m)$, $\mathrm{HH}n(\pm m)$, and $\mathrm{LH}n(\pm m)$ indicate the $n$th electron, heavy-hole, and light-hole states in the $m$th-nearest-neighbor QW from the sixth QW ($m=0$), respectively, and the $+$ $(-)$ sign indicates the QW in the higher (lower) potential side from the sixth QW. In Fig. 1, we find a number of anticrossing behaviors due to the resonant couplings between the WS localization states.

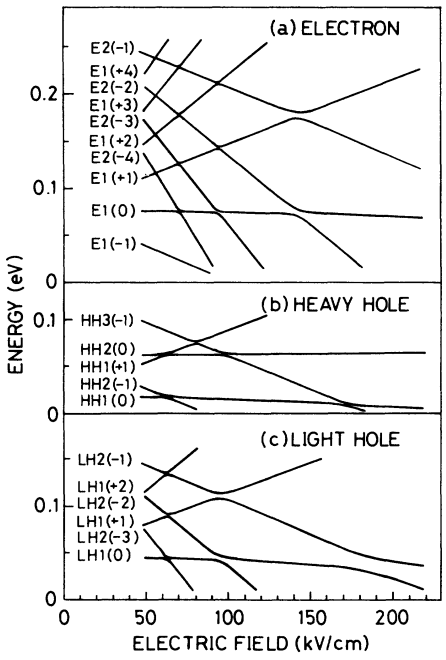


FIG. 1. Calculated energies of the WS localization states of (a) electrons, $En(\pm m)$, (b) heavy holes, $\mathrm{HH}n(\pm m)$, and (c) light holes, $\mathrm{LH}n(\pm m)$ of the GaAs (6.4 nm)/AlAs (0.9 nm) SL as a function of electric field, where $n$ is the quantum number and $m$ is the Stark-ladder index. The energies are measured with respect to the center of the sixth QW corresponding to the center of the modeled SL with the eleven QW's.

In our previous paper,[9] the anticrossing behaviors between the electron subbands are discussed from the splitting features of the ER-line shapes.

In the present paper, we concentrate on the ER-intensity change for the resonant coupling between the WS localization states. It is considered that the ER intensities, which reflect the oscillator strengths of the Stark-ladder transitions, depend on the square of the overlap integral between the WS localization states of electrons and holes. Figure 2 shows (a) the calculated results of the square of the overlap integral between the $n=1$ electron and $n=1$ heavy-hole wave functions in the sixth QW [H11(0)] and (b) those between the $n=1$ electron and $n=1$ light-hole wave functions in the sixth QW [L11(0)] as a function of electric field by using the TM method. From Figs. 1 and 2, it is clear that the square of the overlap integral decreases for the resonant coupling between the WS localization states owing to the wave-function delocalization. The assignments of the resonant couplings are indicated in Fig. 2: e.g., $E1(0)$-$E2(-2)$ denotes the second-nearest-neighbor resonant coupling between the $n=1$ and $n=2$ electron subbands. It is expected that the ER intensity is remarkably reduced for the resonant coupling between the electron subbands and/or for that between the hole subbands. Furthermore, the dip width for the square of the overlap integral reflects the amount of the anticrossing split, which corresponds to the strength of the resonant coupling. The further details will be discussed with the experimental results in the next section.

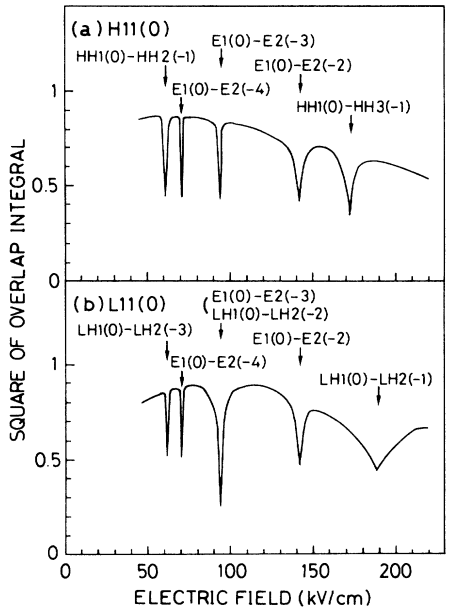


FIG. 2. Calculated values of (a) the square of the overlap integral between the $n=1$ electron and $n=1$ heavy-hole wave functions [H11(0)] and (b) that between the $n=1$ electron and $n=1$ light-hole wave functions [L11(0)] of the GaAs (6.4 nm)/AlAs (0.9 nm) SL as a function of electric field. The assignments of the resonant couplings are indicated by the arrows: e.g., $E1(0)$-$E2(-2)$ denotes the second-nearest-neighbor resonant coupling between the $n=1$ and $n=2$ electron subbands.

## IV. EXPERIMENTAL RESULTS AND DISCUSSION

Figure 3 shows the ER spectra of the GaAs (6.4 nm)/AlAs (0.9 nm) SL at 77 K in the energy range of the heavy-hole and light-hole exciton transitions associated with the $n=1$ subbands at various electric fields $F$ (applied biases $V_b$). The value of the electric field $F$ is estimated from the built-in voltage of 1.64 V of the *p-i-n* structure.[8] The ER spectra are not normalized by reflectance ($R$) because the surface Ohmic electrode prevents us from obtaining the real $R$ signal from the SL. The ER intensity in each spectrum is normalized by that at $F=126$ kV/cm. In previous work,[8,9] we have assigned the ER signals to the Stark-ladder transitions as shown in Fig. 3. The notation of $Hn_1n_2(m)$ [$Ln_1n_2(m)$] for the ER signal represents the transition with the Stark-ladder index $m$ between the $n_1$th electron subband and the $n_2$th heavy-hole (light-hole) subband. In Fig. 3, the ER intensities of the Stark-ladder transitions with $m=\pm1$ decrease remarkably with increasing $F$, which indicates the enhancement of the wave-function localization. The ER signals of the $m=\pm1$ transitions disappear for $F\gtrsim120$ kV/cm, where the value of $eFD$ at $F=120$ kV/cm is about three times as large as the miniband width of the $n=1$ electron state, 30 meV, estimated from the

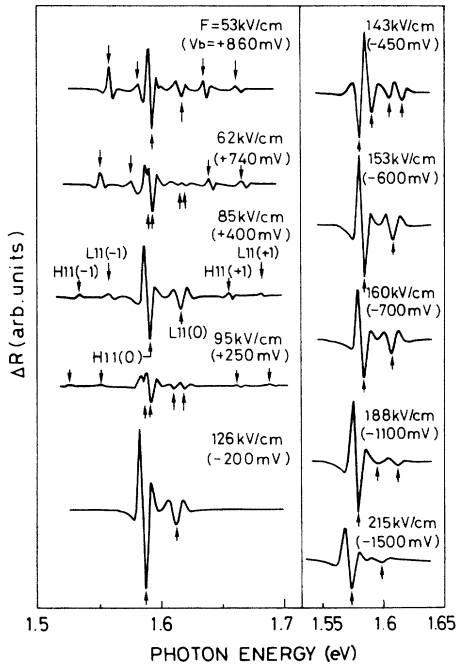


FIG. 3. Electroreflectance spectra of the GaAs (6.4 nm)/AlAs (0.9 nm) SL at 77 K in the energy range of the heavy-hole and light-hole exciton transitions associated with the $n=1$ subbands at various electric fields (applied biases). The electroreflectance intensity in each spectrum is normalized by that at $F=126$ kV/cm. The notation of $Hn_1n_2(m)$ [$Ln_1n_2(m)$] denotes the transition with the Stark-ladder index $m$ between the $n_1$th electron subband and the $n_2$th heavy-hole (light-hole) subband.

effective-mass approximation; therefore, the $n=1$ wave function is fully localized in individual layers.

In Fig. 3, it is found that the ER-line shapes change remarkably with the electric field owing to the various resonant couplings: (1) the appearance of the splitting features of the line shapes due to the formation of the bonding and antibonding states and (2) the intensity reduction due to the wave-function delocalization. The simultaneous changes of the H11(0) and L11(0) signals, which are observed at $F=62$, 95, and 143 kV/cm in Fig. 3, indicate that the resonant coupling between the electron states occurs and/or that the resonant coupling between the heavy-hole states and that between the light-hole states occur simultaneously. In our previous paper,[9] we have indicated that the ER-line-shape changes of the H11(0) and L11(0) transitions at $F=143$ and 95 kV/cm originate from the second- and third-nearest-neighbor resonant couplings between the $n=1$ and $n=2$ electron subbands, respectively. Figure 4 shows the calculated and observed energies of the H11(0) and L11(0) transitions as a function of electric field for the second-nearest-neighbor resonant coupling. The observed energies indicated by the solid (open) circles for the H11(0) [L11(0)] transition are taken from Fig. 3 and our previous report.[9] Since the line-shape-analysis method of the ER signals for the WS localization has not been revealed, we assume that the transition energies correspond to those indicated by the arrows in Fig. 3. The solid (dashed) lines in Fig. 4 indicate the calculated results for the H11(0) and H21(−2) [L11(0) and L21(−2)] transitions, which are shifted down by 10 meV to correct the exciton binding energy. The energies of the splitting ER signals clearly exhibit the anticrossing behavior as a function of electric field, and the experimental results agree with the calculated ones. The ER-line-shape change at $F=62$ kV/cm is due to the simultaneous occurrence of a heavy-hole resonant coupling and a light-hole one, which will be discussed later in detail.

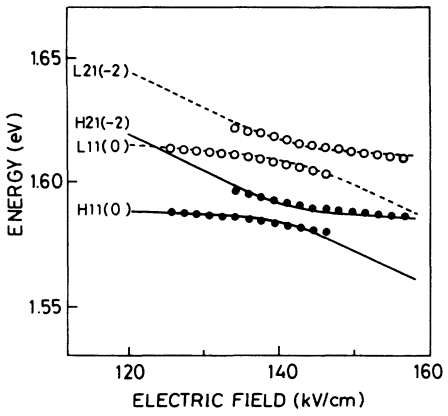


FIG. 4. Energies of the ER signals for the H11(0) and L11(0) transitions indicated by the arrows in Fig. 3 and the calculated energies of the H11(0), H21(−2), L11(0), and L21(−2) transitions as a function of electric field for the second-nearest-neighbor resonant coupling between the $n=1$ and $n=2$ electron subbands.

Noticing the ER spectrum at $F=188$ kV/cm (160 kV/cm) in Fig. 3, only the intensity of the L11(0) [H11(0)] transition is reduced, and the splitting feature of the L11(0) transition is observed. The calculated results of the heavy-hole and light-hole subband energies [Figs. 1(b) and 1(c)] suggest that the intensity reduction of the H11(0) transition at $F=160$ kV/cm and that of the L11(0) transition at $F=188$ kV/cm originate from the first-nearest-neighbor resonant coupling between the $n=1$ and $n=3$ heavy-hole subbands and the coupling between the $n=1$ and $n=2$ light-hole subbands, respectively. For the H11(0) transition under the resonant-coupling condition, we cannot observe the splitting feature of the ER-line shape at $F=160$ kV/cm, which results from the small amount of the anticrossing split, ~2 meV, as shown in Fig. 1(b).

Next, we give a full detail to the ER-intensity change for the resonant coupling between the WS localization states. Figure 5 shows (a) the ER intensity of the H11(0) transition and (b) that of the L11(0) transition as a function of electric field. We assume that the transition intensity corresponds to the amplitude of the ER signal from the peak to the dip. Comparing Fig. 5 with Fig. 2, it is obvious that the electric fields at the dips for the ER intensities in Fig. 5 correspond consistently to those for the square of the overlap integral. The ER-intensity dips are, therefore, assigned to the various resonant couplings on the basis of the calculated results in Fig. 2. The arrows in Fig. 5 indicate the calculated values of the electric fields at which the square of the overlap integral exhibits the

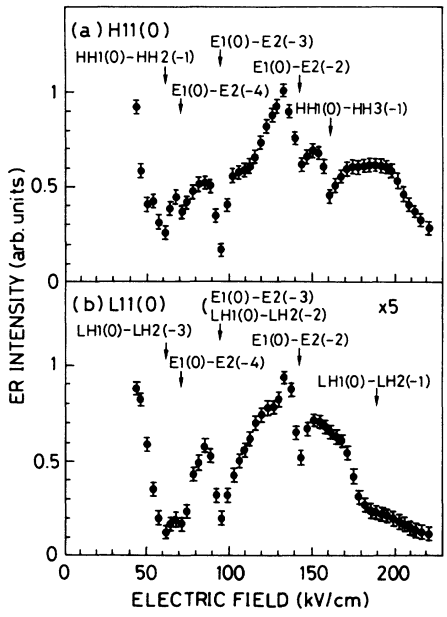


FIG. 5. Electroreflectance intensity of (a) the H11(0) transition and (b) the L11(0) transition as a function of electric field. We assume that the transition intensity corresponds to the amplitude of the electroreflectance signal from the peak to the dip. The arrows indicate the calculated electric fields for the resonant couplings in Fig. 2 except the electric field for the HH1(0)-HH3(−1), which is shifted by 12 kV/cm.

dip profile in Fig. 2 except the electric field for the HH1(0)-HH3(−1) resonant coupling, which is shifted by 12 kV/cm because of the inaccuracy of the calculated energy of the $n=3$ heavy-hole state. The difference in the detailed profile of the ER-intensity change between the calculated and experimental results is because we neglect the exciton effects in the TM calculation: the exciton binding energy and the oscillator strength seem to be remarkably decreased by the wave-function delocalization for the resonant coupling.

For the electron states [see Figs. 5(a) and 5(b)], both the reduction of the ER intensity of the H11(0) transition and that of the L11(0) transition at $F=143$, 95, and 71 kV/cm result from the $E1(0)$-$E2(-2)$, $E1(0)$-$E2(-3)$, and $E1(0)$-$E2(-4)$ resonant couplings, respectively. The electric fields for the second-, third-, and fourth-nearest-neighbor resonant couplings should be in the ratios $\frac{1}{2}:\frac{1}{3}:\frac{1}{4}$ because the $m$th-nearest-neighbor resonant coupling should occur at $eFD=\Delta E_{12}/m$. The experimental results are consistent with the above. Noticing the electric field of 95 kV/cm, the dip width for the ER intensity of the L11(0) transition is broader than that of the H11(0) transition. This is due to the overlap of the two types of the resonant coupling, $E1(0)$-$E2(-3)$ and LH1(0)-LH2(−2). In Fig. 5(a), only the intensity of the H11(0) transition is reduced at $F=160$ kV/cm, which results from the HH1(0)-HH3(−1) resonant coupling. Furthermore, the intensity reduction of the H11(0) transition at $F=62$ kV/cm is due to the HH1(0)-HH2(−1) resonant coupling. In Fig. 5(b), only the intensity of the L11(0) transition is reduced around $F=190$ kV/cm owing to the LH1(0)-LH2(−1) resonant coupling. The intensity reduction of the L11(0) transition at $F=95$ and 62 kV/cm results from the LH1(0)-LH2(−2) and LH1(0)-LH2(−3) resonant couplings, respectively. The electric fields of 190, 95, and 62 kV/cm are in agreement with the expected ratio of $1:\frac{1}{2}:\frac{1}{3}$. It is noted that the intensity reduction of the H11(0) and L11(0) transitions at $F=62$ kV/cm is due to the simultaneous occurrence of the HH1(0)-HH2(−1) and LH1(0)-LH2(−3) resonant couplings. The profile of the ER-intensity change of the L11(0) transition around $F=190$ kV/cm is not the dip-like shape, and both the intensity of the H11(0) transition and that of the L11(0) transition decrease with increasing $F$ for $F\gtrsim 200$ kV/cm. This is due to the quantum-confined Stark effect, which induces the instability of the H11(0) and L11(0) excitons.[23]

Noticing $F\cong 110$ kV/cm in Fig. 5(a) and $F\cong 125$ kV/cm in Fig. 5(b), there are the bends for the ER intensity of the H11(0) and L11(0) transitions, respectively. From the calculated energies of the heavy-hole states [Fig. 1(b)] and the light-hole states [Fig. 1(c)], the energy of the HH1(0) state agrees with that of the LH2(−2) state at $F\cong 110$ kV/cm, and the energy of the LH1(0) state agrees with that of the HH3(−1) state at $F\cong 125$ kV/cm. Therefore, it seems that the bend for the ER intensity of the H11(0) [L11(0)] transition at $F\cong 110$ kV/cm ($\cong 125$ kV/cm) results from the HH1(0)-LH2(−2) [LH1(0)-HH3(−1)] resonant coupling. From the calculated results, it is estimated that the HH1(0)-LH2(−3) resonant coupling takes place at $F\cong 75$ kV/cm; however, we cannot detect it owing to the occurrence of the $E1(0)$-$E2(-4)$ resonant coupling at $F=71$ kV/cm as shown in Fig. 5. Furthermore, the calculated results of the hole-subband energies suggest that the HH1(0)-LH1(−1) and LH1(0)-HH1(+1) resonant couplings occur at $F\cong 35$ kV/cm. Such a low electric field, which corresponds to the high-forward-bias voltage of $\sim 1.13$ V, is out of range of our measurement condition because the large injection current flows through the sample.

## V. CONCLUSIONS

We have systematically measured the ER intensities of the $n=1$ heavy-hole and light-hole exciton [H11(0) and L11(0)] transitions in the GaAs (6.4 nm)/AlAs (0.9 nm) SL as a function of electric field. The ER intensities of the H11(0) and L11(0) transitions are remarkably reduced under the various resonant-coupling conditions between the WS localization states owing to the wave-function delocalization. We have clearly detected the second-, third-, and fourth-nearest-neighbor resonant couplings between the $n=1$ and $n=2$ electron subbands, the first-nearest-neighbor resonant coupling between the $n=1$ and $n=2$ ($n=3$) heavy-hole subbands, and the first-, second-, and third-nearest-neighbor resonant couplings between the $n=1$ and $n=2$ light-hole subbands. Thus, the ER intensity is remarkably sensitive to the resonant coupling. The experimental electric fields for the various resonant couplings consistently agree with the calculated ones by the TM method. On the other hand, the profiles of the ER-intensity changes are explained to some degree by the calculated results of the overlap integral between the electron and hole wave functions. For the precise analysis of the ER-intensity change, we need to consider the exciton effects such as the change of the binding energy and the oscillator strength induced by the wave-function delocalization for the resonant coupling.

## ACKNOWLEDGMENTS

We would like to thank T. Doguchi for his assistance in the measurements. This work was supported in part by Grant-in-Aid (No. 04740176) for Scientific Research from the Ministry of Education, Science and Culture of Japan. One of the authors (I.T.) acknowledges the financial support of the Japan Society for the Promotion of Science for Japanese Junior Scientists.

[1]E. E. Mendez, F. Agulló-Rueda, and J. M. Hong, Phys. Rev. Lett. **60**, 2426 (1988).

[2]P. Voisin, J. Bleuse, C. Bouche, S. Gaillard, C. Alibert, and A. Regreny, Phys. Rev. Lett. **61**, 1639 (1988).

[3]F. Agulló-Rueda, E. E. Mendez, and J. M. Hong, Phys. Rev. B **38**, 12 720 (1988).

[4]K. Fujiwara, Jpn. J. Appl. Phys. **28**, L1718 (1989).

[5]B. Soucail, N. Dupuis, R. Ferreira, P. Voisin, A. P. Roth, D.

Morris, K. Gibb, and C. Lacelle, Phys. Rev. B **41**, 8568 (1990).
[6]H. Schneider, H. T. Grahn, K. v. Klitzing, and K. Ploog, Phys. Rev. Lett. **65**, 2720 (1990).
[7]A. J. Shields, P. C. Klipstein, M. S. Skolnick, G. W. Smith, and C. R. Whitehouse, Phys. Rev. B **42**, 5879 (1990).
[8]M. Nakayama, I. Tanaka, T. Doguchi, H. Nishimura, K. Kawashima, and K. Fujiwara, Solid State Commun. **77**, 303 (1991).
[9]M. Nakayama, I. Tanaka, H. Nishimura, K. Kawashima, and K. Fujiwara, Phys. Rev. B **44**, 5935 (1991).
[10]H. Schneider, K. Kawashima, and K. Fujiwara, Phys. Rev. B **44**, 5943 (1991).
[11]A. M. Fox, D. A. B. Miller, G. Livescu, J. E. Cunningham, and W. Y. Jan, Phys. Rev. B **44**, 6231 (1991).
[12]J. Bleuse, G. Bastard, and P. Voisin, Phys. Rev. Lett. **60**, 220 (1988).
[13]M. M. Dignam and J. E. Sipe, Phys. Rev. B **43**, 4097 (1991).
[14]D. Emin and C. F. Hart, Phys. Rev. B **36**, 7353 (1987); D. A. Page and E. Brown, *ibid.* **43**, 2423 (1991); D. Emin and C. F. Hart, *ibid.* **43**, 2426 (1991); J. Zak, *ibid.* **43**, 4519 (1991); C. F. Hart and D. Emin, *ibid.* **43**, 4521 (1991); J. Leo and A. MacKinnon, *ibid.* **43**, 5166 (1991).
[15]G. Nenciu, Rev. Mod. Phys. **63**, 91 (1991).
[16]B. Soucail, R. Ferreira, G. Bastard, and P. Voisin, Europhys. Lett. **15**, 857 (1991).
[17]I. Bar-Joseph, K. W. Goossen, J. M. Kuo, R. F. Kopf, D. A. B. Miller, and D. S. Chemla, Appl. Phys. Lett. **55**, 340 (1989).
[18]H. Schneider, K. Fujiwara, H. T. Grahn, K. v. Klitzing, and K. Ploog, Appl. Phys. Lett. **56**, 605 (1990).
[19]M. Nido, M. G. W. Alexander, W. W. Rühle, and K. Köhler, Phys. Rev. B **43**, 1839 (1991).
[20]T. B. Norris, N. Vodjdani, B. Vinter, E. Costard, and E. Böckenhoff, Phys. Rev. B **43**, 1867 (1991).
[21]D. C. Hutchings, Appl. Phys. Lett. **55**, 1082 (1989).
[22]D. F. Nelson, R. C. Miller, C. W. Tu, and S. K. Sputz, Phys. Rev. B **36**, 8063 (1987).
[23]D. A. B. Miller, D. S. Chemla, T. C. Damen, A. C. Gossard, W. Wiegmann, T. H. Wood, and C. A. Burrus, Phys. Rev. B **32**, 1043 (1985).